ACS APPLIED MATERIALS & INTERFACES

Research Article

www.acsami.org

Fabrication and Optical Characterization of Silica Optical Fibers Containing Gold Nanoparticles

Rafael E. P. de Oliveira,*[,†,‡] Niclas Sjödin,[‡] Michael Fokine,[§] Walter Margulis,[∥] Christiano J. S. de Matos,[†] and Lars Norin[‡]

[†]Graphene and Nano-Materials Research Center (MackGraphe), Mackenzie Presbyterian University, São Paulo 01302-907, Brazil

[‡]Department Fiber Optics, ACREO Swedish ICT, Hudiksvall SE-824 42, Sweden

[§]Department of Applied Physics, KTH Royal Institute of Technology, Stockholm SE-106 91, Sweden

[∥]Department Fiber Optics, ACREO Swedish ICT, Stockholm SE-164 40, Sweden

Supporting Information

ABSTRACT: Gold nanoparticles have been used since antiquity for the production of red-colored glasses. More recently, it was determined that this color is caused by plasmon resonance, which additionally increases the material's nonlinear optical response, allowing for the improvement of numerous optical devices. Interest in silica fibers containing gold nanoparticles has increased recently, aiming at the integration of nonlinear devices with conventional optical fibers. However, fabrication is challenging due to the high temperatures required for silica processing and fibers with gold nanoparticles were solely demonstrated using sol−gel techniques. We show a new fabrication technique based on standard preform/fiber fabrication methods, where nanoparticles are nucleated by heat in a furnace or by laser exposure with unprecedented control over particle size, concentration, and distribution. Plasmon absorption peaks exceeding 800 dB m^{-1} at 514−536 nm wavelengths were observed, indicating higher achievable nanoparticle concentrations than previously reported. The measured resonant nonlinear refractive index, $(6.75 \pm 0.55) \times 10^{-15}$ m^2 W^{-1}, represents an improvement of >50×.

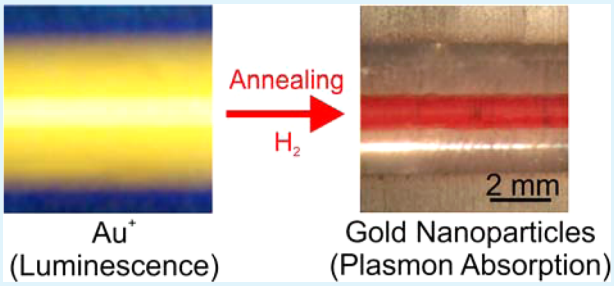

KEYWORDS: *gold nanoparticles, plasmonics, nanoparticles in glass, specialty optical fibers, nonlinear optics*

INTRODUCTION

Nonlinear optical effects are essential to numerous optical devices, such as modulators, switches, amplifiers, pulse shapers, frequency converters, and broadband sources.[1,2] The development of such devices based on optical fibers may improve their integration with conventional transmission fibers, reducing insertion loss and improving the ruggedness of optical systems. Nonlinear effects are highly favored in the optical fibers geometry due to the high intensity of light confined to small areas in long interaction lengths. Conventional optical fibers[3] and photonic crystal fibers (PCFs) have been successfully used for nonlinearity-based applications.[1,4] These fibers are usually made up of silica glass, which provides good mechanical and linear optical properties but has the disadvantage of a relatively low nonlinear refractive index,[2] $n_2 \sim 2 \times 10^{-20}$ m^2 W^{-1}. This drawback can be partially compensated for by designing optical fibers with small cores to increase the light intensity, for instance, exploiting the tight confinement possible in PCFs. However, those microstructures reduce the compatibility with standard fibers, causing higher coupling losses due to the difference between fiber cross sections.[5] The search for higher nonlinear materials for optical fibers is also motivated by the chromatic dispersion that limits the effective length of processes requiring phase-matching for momentum conservation, such as frequency conversion and amplification through four-wave mixing.[2] Dispersive effects can be minimized in shorter pieces of fiber with higher nonlinearity.[6]

Alternative materials such as chalcogenide glasses have been investigated for nonlinear optical fiber applications and exhibit nonlinear coefficients 2 orders of magnitude higher than that of silica.[7] These materials are, however, incompatible with standard silica-based fibers in terms of splicing and refractive index mismatch and also show losses that are hundreds of times larger than those of silica, particularly in the near-infrared and visible regions.[7]

A promising approach for the envisioned applications is the use of silica glass fibers with nonlinear response increased by the addition of metallic nanoparticles.[8] The increased nonlinearity in glasses containing metallic nanoparticles is well-known,[9−16] and silica glasses with resonant nonlinear refractive indices as high as $n_2 \sim 10^{-12}$ m^2 W^{-1}, which is 8 orders of magnitude larger than pure silica, have been reported.[11] This increased nonlinearity is strongest near the surface plasmon resonance (SPR) frequency, where the incident optical electric

Received: September 16, 2014
Accepted: December 10, 2014
Published: December 10, 2014

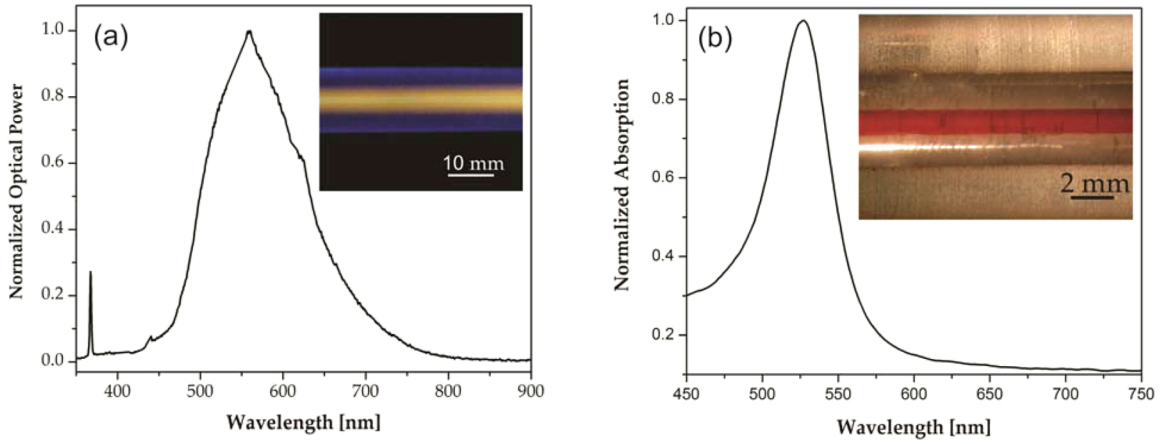

Figure 1. Preform before and after nanoparticle formation. (a) Preform luminescence spectrum due to gold ions before nanoparticle growth and (inset) side view of the preform under UV illumination. (b) Preform absorption spectrum after annealing and nanoparticle growth and (inset) side view of the preform with a red-colored core.

field excites collective harmonic oscillation on the surface of the nanoparticles. For spherical gold nanoparticles embedded in silica with diameters much smaller than the light wavelength, SPR occurs at around 530 nm excitation wavelength. At plasmon resonance, the electric field increases locally, which improves the material nonlinear response.[8,9] Other contributions to the increase in nonlinearity come from electron transition from d valence to the s-p conduction band, with a femtosecond response time and a slower thermal contribution with a nanosecond response time. The response time for SPR is in the picosecond time-scale,[8−10,15] which is suitable for fast switching applications.

The growth of gold nanoparticles in silica glass is, however, challenging due to the high temperatures required for manufacturing silica-based fibers (~2000 °C) and the poor solubility of gold. For this reason, gold nanoparticles in silica are usually obtained in thin layers, produced by sputtering or ion implantation;[10,14] in softer glasses such as sodium- or lead-doped silicate glasses;[15,17] or by sol−gel fabrication processes for silica glass,[10,12] a nonconventional technique for optical fiber fabrication that is more prone to contamination in the final glass.

The fabrication of silica optical fibers containing nanoparticles has attracted attention recently.[18−20] Ju et al. demonstrated a fiber containing gold nanoparticles fabricated using sol−gel followed by solution doping techniques in a germanium-doped core fiber.[18] It is pointed out that the tetraethyl-orthosilicate used in the sol−gel process plays an important role in reducing the gold and forming gold nanoparticles.[21] The resulting fiber presented an SPR peak at 490 nm with 1.7 dB m^{-1} absorption. The observed blue-shift in plasmon resonance relative to the expected wavelength is not clearly explained, as also pointed out by Bigot.[19] The nonlinear refractive index was measured to be $n_2 = 1.27 \times 10^{-16}$ m^2 W^{-1} at 488 nm wavelength.[21]

Also using a sol−gel technique, Bigot et al. fabricated a photonic crystal fiber containing gold nanoparticles.[19] This fiber showed an SPR peak at 522 nm with 5 dB m^{-1} attenuation. The maximum attenuation was estimated to be 300 dB m^{-1} by accounting for the small overlap between the optical field and the gold nanoparticles' doped region. The nonlinear absorption coefficient was measured to be $\beta = 0.84 \times 10^{-14}$ m W^{-1}.

Halder et al. described germanium- and aluminum-doped silica fibers containing silver nanoparticles[20] fabricated by MCVD and solution doping techniques and made use of a He-rich environment to avoid silver oxidation during both drying and preform sintering steps. The fiber presented an SPR peak at 395 nm with 36 dB m^{-1} attenuation. However, nonlinearity was not characterized, and applications were focused on the use of the luminescence for lasing and optical amplification.

All the processes described above give little control over particle size and distribution, because particles are grown during the preform fabrication, but the nanoparticle characteristics are ultimately determined by the temperatures associated with fiber drawing. Here, we present a technique to fabricate optical fibers where the gold nanoparticles can be nucleated and grown in the fiber after the drawing process, allowing for unprecedented control over nanoparticles size, density, and distribution. The nanoparticles can also be formed in the preform before fiber drawing, resulting in larger particles than those demonstrated with sol−gel based techniques. The choice of gold over silver was due to the advantage of having the SPR at longer wavelengths where silica has lower loss and lasers are more readily available. The fiber nonlinear response was characterized in the continuous wave and slow transient regimes.

PREFORM FABRICATION

The fiber fabrication started with a pure silica preform tube where a layer of porous silica was deposited on the inner wall by MCVD. This layer was soaked at room temperature for 2 h in a solution containing the dopant precursors, in the standard technique of solution doping.[18,20] The preform was doped in two steps: first, with a solution of $Au(OH)_3$ (Aldrich, 99.9%) in concentrated nitric acid (Merck, 65% HNO_3, p.a. grade), aiming at a 300 ppm concentration of gold in glass; and second, with $AlN_3O_9{\cdot}9H_2O$ (Aldrich, 99.997%) dissolved in ultrapure water (Milli-Q), aiming at ~7 mol % of aluminum in glass. After each soaking step, the preform was dried at 400 °C for 2 h. After soaking and drying, the preform was collapsed in 100% oxygen, and the optical fiber was drawn.

Aluminum was used to increase the refractive index of the core and to favor the dissolution of gold ions in glass. Without aluminum, the gold precursor decomposes to metallic gold during the preform collapse, creating large gold clusters that obstruct the collapse. Gold dissolution is favored by aluminum

dx.doi.org/10.1021/am506327q | ACS Appl. Mater. Interfaces 2015, 7, 370−375

codoping because aluminum atoms substitute silicon atoms in the glass structure and form negative sites in the glass matrix due to their lower oxidation state. Gold ions (Au^+) locally coordinate to AlO_4^- sites for charge compensation.[18]

After the doping and subsequent collapse, the preform is transparent throughout the visible and near-infrared spectra. A strong yellow luminescence centered at 557 nm was observed in the preform when excited by a mercury UV-lamp. The luminescence spectrum is shown in Figure 1a, and the corresponding optical image of the yellow glowing preform in the inset; the sharp peak observed in the spectrum at ~367 nm is reminiscent of the excitation light. Although previously unreported for gold dissolved in glass, this luminescence can be attributed to Au^+ ions.[22,23] The luminescence was also observed in the cladding, outside the doped core region, due to the high diffusivity of gold ions in the silica glass during the high temperatures used in the final steps of preform processing (1800–2000 °C). This diffusion has little impact on the final fiber profile because most of the gold stays in the core.

NANOPARTICLE GROWTH BY THERMAL ANNEALING

At this point, the nanoparticles can be nucleated through annealing the preform in a furnace at reducing atmosphere conditions. Annealing at 850 °C for 24 h in an atmosphere of 5 vol % H_2/95 vol % N_2 resulted in gold nanoparticles in the preform that exhibited the characteristic red color shown in the inset of Figure 1b. The red color in the core region is due to the nanoparticles' plasmon absorption spectrum, which peaks at 527 nm, as shown in Figure 1b. At this point, the yellow luminescence is no longer observed due to the reduction of the gold ions by the hydrogen. The presented technique is very robust and reproducible; five preforms were fabricated with different concentrations of gold (100–1000 ppm) and aluminum (7–10.1 mol %) and those variables have proven noncritical to the nanoparticle formation process, allowing the control of the nanoparticle concentration and fiber core refractive index from the initial dopant levels.

Nanoparticles with a spherical shape are expected due to the isotropic structure of the glass and to the uniform temperature and atmospheric conditions used for their formation; the nanoparticle's shape was later confirmed by transmission electron microscopy (TEM) images captured in similarly produced preforms. Mie's theory,[24] which relates the plasmon absorption peak in spherical particles to their diameter, was used to estimate the mean nanoparticle size. This theory is usually based on bulk gold's permittivity values, which are not valid for particle diameters smaller than ~20 nm[25−27] due to the proximity with the electron mean free path value[8] and to quantum effects becoming more significant in the particle.[9,25] These effects were considered in a model using a size-dependent gold's permittivity calculation that is based on that reported by Scholl et al.[25] (Supporting Information). According to the model the observed peak wavelength at 527 nm in the preform corresponds to a nanoparticle diameter of 18 nm. This model is used to estimate the particle size in all cases shown in this paper.

The preform containing gold nanoparticles was drawn to an optical fiber with dimensions similar to those of standard telecom fibers (125 μm outer diameter and ~10 μm core diameter). The resulting absorption spectrum is shown in Figure 2 and identified as Fiber 1. A red shift in the plasmon absorption peak (centered at 536 nm) can be noticed relative

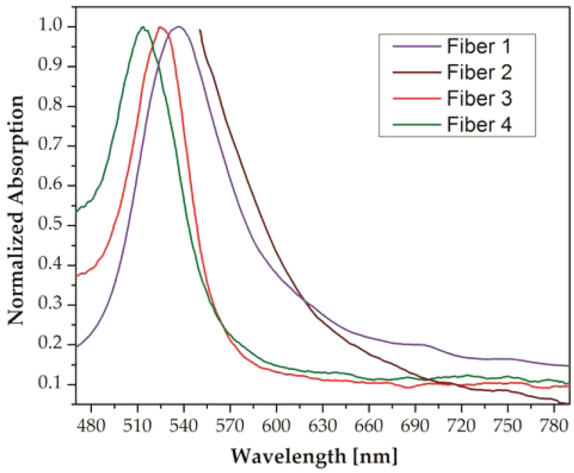

Figure 2. Normalized plasmon resonance absorption spectra for fibers with nanoparticles nucleated via different processes. Fiber 1: nanoparticles nucleated in the preform stage (peak at 536 nm). Fiber 2: nanoparticles nucleated in the fiber. Fiber 3: one-step nucleation with a CO_2 laser (peak at 526 nm). Fiber 4: two-step nucleation with a CO_2 laser (peak at 514 nm).

to the preform spectrum, which is due to the particle growth in the high temperatures, near 2000 °C, required for fiber drawing. The mean particle size was estimated to be around 40 nm in diameter (Figure S1, Supporting Information). However, fluctuations related to the preform process resulted in lengths of fiber with higher concentrations of gold clusters that were highly scattering, in which light was expelled from the core to the cladding within a few centimeters of propagation. Fine tuning of the doping and collapsing procedures are required for obtaining fibers with a more consistent distribution of nanoparticles.

Better control over particle growth can be achieved by creating nanoparticles directly in the drawn fiber. To this end, the preform is drawn before the annealing stage, creating a fiber with dissolved gold ions. At this point, no spectral features were observed and the attenuation was measured to be 1 dB m^{-1} at 1510 nm. The gold ions in the fiber can then be reduced to nucleate and grow nanoparticles in a similar way as for the preform in the earlier case. This method allows for a better control of the particle size because the subsequent ~2000 °C heating is not required. One fiber was annealed in reducing atmosphere for 3 h at 780 °C and the resulting particle size was estimated to be ~15 nm, which is similar to the case for nanoparticles formed in the preform because the reduction and growth conditions are similar in both cases and considering the lower temperature used in the fiber. The high gold concentration resulted in fibers with much higher absorption compared to previously reported in the literature; with peak absorptions well in excess of 800 dB m^{-1} (the exact value could not be determined with our cut-back measurement setup). Figure 2 shows the absorption spectrum identified as Fiber 2 down to 550 nm, beyond which the absorption exceeds 750 dB m^{-1}. Assuming that the particle growth process is similar to that taking place in the preform annealing process, the absorption peak is expected to be around 525 nm (Figure 1b). The attenuation at 1510 nm was measured and increased to 6 dB m^{-1} after gold nanoparticle growth, a small penalty given the high concentration of nanoparticles. In all cases, the fiber was fully spliceable to conventional fibers using a standard fusion splicer.

dx.doi.org/10.1021/am506327q | ACS Appl. Mater. Interfaces 2015, 7, 370−375

NANOPARTICLE GROWTH USING A CO_2 LASER BEAM

Besides annealing in a furnace before or after the fiber is drawn, an alternative nanoparticle growth process was developed, which consists of exposing a hydrogenated fiber to local heating using a CO_2 laser. This technique allows for better control over particle size, concentration and, most importantly, the spatial distribution of the nanoparticles can be controlled by the laser beam spot. Particle growth over longer sections can be achieved by scanning the laser along the fiber, thus enabling fiber customization for each application. The fibers were preloaded with hydrogen at 90 °C under a 120 bar for 10 h to provide reducing conditions. Fiber sections were subsequently heated by focusing the CO_2 laser beam on the fiber side and by scanning the beam along a 25 mm length at a ~1.3 mm s^{-1} speed. For further nanoparticle nucleation and growth, the scan could be repeated several times. This technique allows a resolution for nanoparticles nucleation of ~100 μm in fiber length. The temperature in the heated fiber section was calibrated using the spectral shift of the reflective peak of thermally stable Bragg gratings.[28]

Figure 3 shows the SPR spectra for a fiber heated to 1250 °C by the CO_2 laser. The absorption peak increases for each scan along the 25 mm fiber length, indicating, according to Mie's theory, a gradual growth of the nanoparticle concentration and size. After the ninth scan, the absorption peak reached 450 dB m^{-1} attenuation and after the 14th scan (not shown) the peak absorption exceeded 800 dB m^{-1}. The absorption peak shifted from 505 to 532 nm from the second to the twelfth scan which is believed to indicate particle size growth (Figure 3, inset). The normalized absorption spectrum after the ninth scan is shown in Figure 2 and is identified as Fiber 3. The peak around 526 nm indicates a particle diameter of ~16 nm, and the peak at 532 (not shown in the graph) indicates a mean particle diameter close to ~30 nm (Figure S1, Supporting Information).

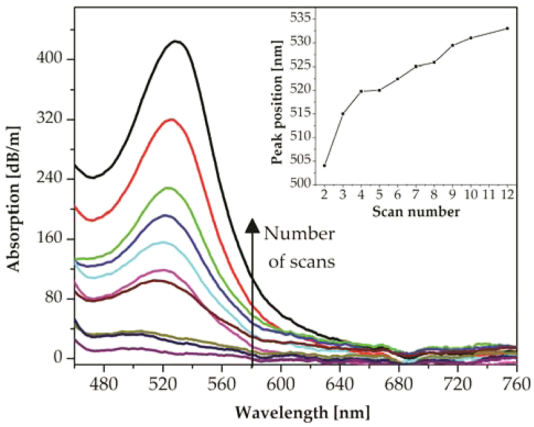

Figure 3. Absorption spectra for a 25 mm section of fiber heated by a scanned CO_2 laser beam. The concentration and size of the gold nanoparticles increase gradually with the number of scans along the fiber. (Inset) Absorption peak position as the scan number function.

Heating the hydrogen loaded fiber provides energy for the reduction of gold ions, as well as increases the mobility of gold ions and atoms. We believe that in each scan of the CO_2 laser both processes of reduction and coalescence occur, resulting in the controlled growth of the nanoparticles' size and concentration per scan. However, the temperature ranges that favor particle growth and nucleation are not the same. Gold reduction and particle growth tend to increase as temperature increases, while the nucleation rate tends to decrease. Furthermore, higher temperatures also favor hydrogen out-diffusion, effectively terminating the reduction process. To improve the efficiency of the nucleation step, we split the process into two stages. First, the temperature (i.e., the laser power) was lowered to enhance the nucleation rate. A temperature of 850 °C was used, and three scans were performed. No nanoparticle formation could be observed. After this first heating stage, a second heating was performed at a higher temperature (1350 °C) to grow the nanoparticles. Because the gold ions were already efficiently reduced and nucleated in the first step, the gold nanoparticles grew rapidly, and after a single scan, the plasmon absorption peak reached 800 dB m^{-1} at 516 nm, with an estimated particle size of ~6 nm. The shorter peak wavelength position compared to a similar absorption level in the previous case is due to the formation of a higher number of smaller particles in such conditions. When the temperature was reduced to 800 °C in the first heating stage, the SPR absorption peak wavelength (after the second stage) was shifted to 514 nm, meaning that even smaller particles of ~5 nm were formed after a single scan. The absorption spectrum for this case is shown in Figure 2 and is identified as Fiber 4.

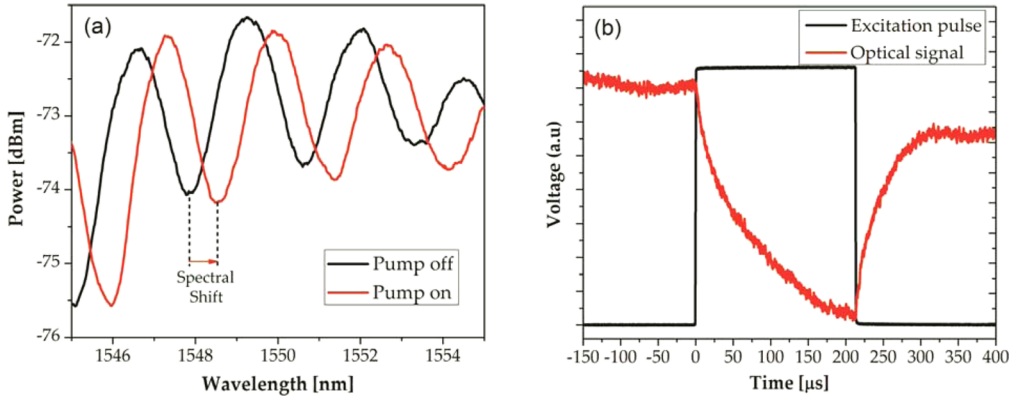

Figure 4. Nonlinear optical response. (a) Mach–Zehnder interference spectrum in the NP fiber around 1550 nm and spectral shift due to nonlinear effects with a 60 mW pump at 650 nm. (b) Temporal response when the signal is fixed at 1550 nm and a 30 mW pump is modulated by a chopper.

dx.doi.org/10.1021/am506327q | ACS Appl. Mater. Interfaces 2015, 7, 370–375

Controlling the temperatures in the two-stage heating process allows for the control of the particle size, creating conditions for faster growth of smaller nanoparticles (shorter plasmon absorption wavelengths) compared to the single stage heating, using only a single high-temperature step. The single stage method, on the other hand, allows for a finer control over the particle concentration (because the nucleation is slower) and for the formation of larger particles (longer plasmon absorption wavelengths). With both techniques, highly concentrated gold nanoparticles with resonances ranging from 514 to 532 nm were achieved in optical fiber sections, which correspond to particles estimated from 5 to 30 nm in diameter.

NONLINEAR OPTICAL CHARACTERIZATION

The optical nonlinearity of fiber sections containing gold nanoparticles was characterized using a technique similar to that used by Ju et al. and Kim et al.[21,29] The experimental setup is detailed and shown in Figure S2 (Supporting Information). An interferometer formed between core and cladding modes in a 12 cm long section of Fiber 2 (Figure 2) was used. A broadband amplified spontaneous emission (ASE) around 1550 nm from an erbium-doped fiber was coupled into the NP fiber and the output spectrum was monitored in an optical spectrum analyzer (OSA). The obtained interference pattern is shown in Figure 4a. A continuous wave (CW) laser at 650 nm near the plasmon resonance peak was used as the pump source. At its wavelength, which is close to the plasmon absorption, the fiber attenuation was 76 dB m^{-1}. The pump induces a nonlinear change in the refractive index that shifts the interference pattern as shown in Figure 4a, for a 60 mW coupled pump power. From the spectral shift one can calculate the nonlinear refractive index of the fiber[21,28] to be $n_2 = (6.75 \pm 0.55) \times 10^{-15}$ m^2 W^{-1}, which is 5 orders of magnitude higher than that of pure silica and 50 times higher than previously reported for a fiber containing gold nanoparticles using CW pumping.[21] The higher nonlinear refractive index achieved in our case can be explained by a higher concentration of gold nanoparticles, and the improvement is even higher considering that in the measurement reported by Ju et al.[21] the pump wavelength was closer to the plasmon absorption peak.

The time response of the optical nonlinearity was measured using a chopper to modulate the pump, creating square pulses of 220 μs duration. In this case, the signal was a tunable laser with wavelength set to 1550 nm, corresponding to the quadrature point with maximum derivative in the interference spectrum. The nonlinear response was found to be dominated by a slow response in the microsecond (μs) time scale, as shown in Figure 4b. This feature is expected because the thermal response is known to dominate when nanoparticles are excited under CW or quasi-CW conditions.[9−11] Although the thermal diffusion in nanoparticles is in the nanosecond scale,[10,11] the time response is determined by heat diffusion in the silica matrix.[30] A characterization with a picosecond duration pump would be required for inferring the fast, electronic, nonlinear component because the surface plasmon dynamics occurs in this time-scale when the thermal response is minimized.[10,11]

CONCLUSIONS

Optical fibers containing metallic nanoparticles are promising components for future nonlinear optical devices, in which plasmonic effects can be exploited. Here, we show a new technique for the fabrication of such fibers, through doping with gold ions and the subsequent ion reduction and growth of gold nanoparticles. The fiber is silica based, allowing for complete integration with standard telecommunications optical fibers. Particle nucleation and growth could be achieved via annealing the preform before drawing or by postannealing the fiber. In the latter case, the annealing could be obtained in a furnace or locally, with ~100 μm resolution, through heating with a CO_2 laser beam. Such a variety of particle growth methods in optical fibers allows for unprecedented control over particle size and concentration, with the corresponding plasmon resonance peaking at wavelengths ranging from 514 nm up to 536 nm. The nonlinear optical response was characterized in a regime favorable to its thermal component, with a nonlinear refractive index measured that is 50× higher than those previously reported. Further investigations using a picosecond pulse pump laser will determine the fast nonlinear response component that is also expected to be increased relative to conventional fibers.

ASSOCIATED CONTENT

Supporting Information

Model used for nanoparticle plasmon resonance calculation and experimental setup for nonlinear characterization. This material is available free of charge via the Internet at http://pubs.acs.org.

AUTHOR INFORMATION

Corresponding Author

*E-mail: repdeoliveira@gmail.com.

Author Contributions

The manuscript was written through contributions of all authors. All authors have given approval to the final version of the manuscript. R.d.O. fabricated the fiber and participated in all experiments. N.S., W.M., and L.N. contributed in fiber development and fabrication. C.d.M. participated in the experiments of nucleation with CO_2 laser beam and of nonlinear characterization. M.F. participated in the experiments of nucleation with CO_2 laser beam.

Funding

This work was supported by FAPESP (grant. n° 2012/50259-8), CAPES (scholarship n° 6275/11−7), CAPES-STINT project, INCT Fotonicom, CNPq, and MackPesquisa. It was partially carried out within Acreo Fiber Optic Center, partly funded by the Swedish Foundation for Strategic Research within the ProInstitute Program.

Notes

The authors declare no competing financial interest.

ACKNOWLEDGMENTS

Acknowledgements to Håkan Olsson, Mats Eriksson, Björn Byström, and Helena Eriksson-Quist for their contributions in the fiber fabrication process and to Gerson K. Sinohara for his assistance in the experiments involving heating by laser beam.

REFERENCES

(1) Agrawal, G. P. Nonlinear Fiber Optics: Its History and Recent Progress. *J. Opt. Soc. Am. B* **2011**, *28*, A1−A10.

(2) Boyd, R. W. *Nonlinear Optics*, 2nd ed; Academic Press: San Diego, CA, 2003.

(3) Stolen, R. H. The Early Years of Fiber Nonlinear Optics. *J. Lightwave Technol.* **2008**, *26*, 1021−1031.

(4) Coen, S.; Hing, A.; Chau, L.; Leonhardt, R.; Harvey, J. D.; Knight, J. C.; Wadsworth, W. J.; Russel, P.; St, J. White-Light Supercontinuum Generation with 60-ps Pump Pulses in a Photonic Crystal Fiber. *Opt. Lett.* **2001**, *26*, 1356−1358.
(5) Xiao, L.; Jin, W.; Wang, Y.; Zhao, C.-L. Fusion Splicing Photonic Crystal Fibers and Conventional Single-Mode Fibers: Microhole Collapse Effect. *J. Lightwave Technol.* **2007**, *25*, 3563−3574.
(6) Sharping, J. E. Microstructure Fiber Based Optical Parametric Oscillators. *J. Lightwave Technol.* **2008**, *26*, 2184−2191.
(7) Eggleton, B. J.; Luther-Davies, B.; Richardson, K. Chalcogenide Photonics. *Nat. Photonics* **2011**, *5*, 141−148.
(8) Stockman, M. I. Nanoplasmonics: Past, Present, and Glimpse into Future. *Opt. Express* **2011**, *19*, 22029−22106.
(9) Yamane, M.; Asahara, Y. *Glasses for Photonics*; Cambridge University Press: Cambridge, 2004.
(10) Compton, D.; Cornish, L.; van der Lingen, E. The Third Order Nonlinear Optical Properties of Gold Nanoparticles in Glasses, Part I. *Gold Bull. (Berlin, Ger.)* **2003**, *36*, 10−16.
(11) Liao, H. B.; Xiao, R. F.; Fu, J. S.; Wang, H.; Wong, K. S.; Wong, G. K. L. Origin of Third-Order Optical Nonlinearity in Au:SiO_2 Composite Films on Femtosecond and Picosecond Time Scales. *Opt. Lett.* **1998**, *23*, 388−390.
(12) Muto, S.; Kubo, T.; Kurokawa, Y.; Suzuki, K. Third-Order Nonlinear Optical Properties of Disperse Red 1 and Au Nanometer-Size Particle-Doped Alumina Films Prepared by the Sol−Gel Method. *Thin Solid Films* **1998**, *322*, 233−237.
(13) Monteiro-Filho, J. B.; Gómez-Malagón, L. A. Resonant Third Order Nonlinear Optical Susceptibility of Gold Nanoparticles. *J. Opt. Soc. Am. B* **2012**, *29*, 1793−1798.
(14) Stepanov, A. L. Nonlinear Optical Properties of Implanted Metal Nanoparticles in Various Transparent Matrix: A Review. *Rev. Adv. Mater. Sci.* **2011**, *27*, 115−145.
(15) Hache, F.; Ricard, D.; Flytzanis, C. Optical Nonlinearities of Small Metal Particles: Surface-Mediated Resonance and Quantum Size Effects. *J. Opt. Soc. Am. B* **1986**, *3*, 1647−1655.
(16) Takeda, Y.; Plaksin, O. A.; Kishimoto, N. Dispersion of Nonlinear Dielectric Function of Au Nanoparticles in Silica Glass. *Opt. Express* **2007**, *15*, 6010−6018.
(17) Wagner, F. W.; Haslbeck, S.; Stievano, L.; Calogero, S.; Pankhurst, Q. A.; Martinek, K.-P. Before Striking Gold in Gold-Ruby Glass. *Nature* **2000**, *407*, 691−692.
(18) Ju, S.; Nguyen, V. L.; Watekar, P. R.; Kim, B. H.; Jeong, C.; Boo, S.; Kim, C. J.; Han, W.-T. Fabrication and Optical Characteristics of a Novel Optical Fiber Doped with Au Nanoparticles. *J. Nanosci. Nanotechnol.* **2006**, *l6*, 3555−3558.
(19) Bigot, L.; Hamzaoui, H. E.; Rouge, A. L.; Bouwmans, G.; Chassagneux, F.; Capoen, B.; Bouazaoui, M. Linear and Nonlinear Optical Properties of Gold Nanoparticle-Doped Photonic Crystal Fiber. *Opt. Express* **2011**, *19*, 19061−19066.
(20) Halder, A.; Paul, M. C.; Das, S.; Pal, M.; Bhadra, S. K.; Bysakh, S.; Martínez-Gamez, A. M.; Garcia, V.; Lucio-Martínez, J. L.; Kir'yanov, A. V. Experimental Study of Metal Nanoparticle Doped Optical Fiber and its Unique Spectral Property. In *OSA Technical Dig.*, Proceedings of the International Conference in Fiber Optics and Photonics, Chennai, India, Dec 9−12, 2012; The Optical Society: Washington, DC, **2012**; paper M3B.4.
(21) Ju, S.; Watekar, P. R.; Kang, S. G.; Chung, J.-K.; Kim, C. J.; Han, W.-T. Effect of TEOS Addition on Formation of Au Metal Nanoparticles in the Au-Doped Optical Fiber and its Optical Nonlinearity. *J. Non-Cryst. Solids* **2010**, *356*, 2578−2582.
(22) Zhou, C.; Sun, C.; Yu, M.; Qin, Y.; Wang, J.; Kim, M.; Zheng, J. Luminescent Gold Nanoparticles with Mixed Valence States Generated from Dissociation of Polymeric Au (I) Thiolates. *J. Phys. Chem. C* **2010**, *114*, 7727−7732.
(23) Zheng, J.; Zhou, C.; Yu, M.; Liu, J. Different Sized Luminescent Gold Nanoparticles. *Nanoscale* **2012**, *4*, 4073−4083.
(24) Hergert, W.; Wriedt, T. *The Mie Theory Basics and Applications*; Springer: Berlin, 2012.
(25) Scholl, J. A.; Koh, A. L.; Dionne, J. A. Quantum Plasmon Resonance of Individual Metallic Nanoparticles. *Nature* **2012**, *483*, 421−428.
(26) Stoller, P.; Jacobsen, V.; Sandoghdar, V. Measurement of the Complex Dielectric Constant of a Single Gold Nanoparticle. *Opt. Lett.* **2006**, *31*, 2474−2476.
(27) Haiss, W.; Thanh, N. T. K.; Aveyard, J.; Fernig, D. G. Determination of Size and Concentration of Gold Nanoparticles from UV−Vis Spectra. *Anal. Chem.* **2007**, *79*, 4215−4221.
(28) Holmberg, P.; Fokine, M. Thermometric Study of CO_2-Laser Heated Optical Fibers in Excess of 1700 °C Using Fiber Bragg Gratings. *J. Opt. Soc. Am. B* **2013**, *30*, 1835−1842.
(29) Kim, Y. H.; Lee, B. H.; Chung, Y.; Paek, U. C.; Han, W.-T. Resonant Optical Nonlinearity Measurement of Yb^{3+}/Al^{3+} Codoped Optical Fibers by use of a Long-Period Fiber Grating Pair. *Opt. Lett.* **2002**, *27*, 580−582.
(30) Rugeland, P.; Tarasenko, O.; Margulis, W. Nanosecond Monolithic Mach−Zehnder Fiber Switch. *Opt. Express* **2012**, *20*, 29309−29318.